

PAPER • OPEN ACCESS

Evolution of microstructure and mechanical properties of Ti-based metal-matrix composites during high-pressure torsion

To cite this article: M S Ozerov *et al* 2019 *IOP Conf. Ser.: Mater. Sci. Eng.* **672** 012034

View the [article online](#) for updates and enhancements.

Evolution of microstructure and mechanical properties of Ti-based metal-matrix composites during high-pressure torsion

M S Ozerov¹, M V Klimova¹, E A Shigoleva¹, T N Vershinina², Yu V Ivanisenko³
N D Stepanov¹ and S V Zhrebtsov¹

¹ Laboratory of Bulk Nanostructured Materials, Belgorod National Research University, Belgorod 308015, Russia

² Centre of Nanostructured Materials and Nanotechnology, Belgorod State University, Belgorod 308015, Russia

³ Karlsruhe Institute of Technology, Institute of Nanotechnology, Karlsruhe 76021, Germany

E-mail: Zhrebtsov@bsu.edu.ru

Abstract. The microstructure and microhardness evolution of a Ti/TiB and Ti-15(wt.%)Mo/TiB metal-matrix composites (MMC) during high-pressure torsion (HPT) at 400 °C was studied. The composites were fabricated by spark plasma sintering of either hcp α -Ti with 10 wt.% of TiB₂ or Ti with 13.5 wt.% of Mo (resulted in a bcc β -Ti matrix) and of 10 wt.% TiB₂ powders mixtures at 1000 or 1200 °C, respectively. An increase in the dislocation density, a considerable decrease in the grain size in both hcp or bcc Ti matrix, and shortening of TiB whiskers were observed in the microstructures of the composites during HPT. After five revolutions, a nanostructure with a (sub) grain size of ~30 or ~55 nm was produced in Ti or Ti-15Mo matrix, respectively. The microhardness increased with strain from 452 HV in the initial state to 520 HV after 5 revolutions for Ti/TiB MMC and from 575 to 730 HV for Ti-15Mo/TiB MMC. The contributions of various hardening mechanisms to the composites were evaluated.

1. Introduction

One of the well-known ways to increase strength of metallic materials is associated with a significant microstructure refinement through severe plastic deformation (SPD) [1, 2]. Due to a considerable decrease in grain size, commercially pure titanium, for example, becomes strong enough for production of surgical implants [3]. Another promising approach to increase strength of titanium without losing its biocompatibility or high corrosion properties can be associated with embedding of ceramic reinforcements, like TiB, in titanium matrix [4, 5]. SPD of such metal-matrix composites (MMCs) induces therefore the simultaneous operation of several hardening mechanisms (substructure hardening, Hall–Petch strengthening, precipitation hardening by TiB fibers) [6].

Some additional hardening mechanisms (solid solution hardening or strengthening due to the formation of ω -phase particles or twins) may also be involved as a result of the transition of the titanium matrix from the hcp α -phase to the bcc β -phase. This transition can be attained by alloying of the titanium matrix with Mo, which is a strong beta-stabilizing element.

In the present work, Ti/TiB and Ti-15(wt.%)Mo/TiB MMCs were fabricated through a spark plasma sintering process (SPS). Then, the composites were deformed using high-pressure torsion



(HPT) at 400 °C to different strain levels [7]. The microstructure evolution of the composites was comprehensively studied using X-ray diffraction (XRD), scanning (SEM) and transmission electron microscopy (TEM); microhardness was measured to evaluate the influence of HPT on their mechanical properties.

2. Materials and methods

Commercial purity powders of Ti (99.1% purity), Mo (99.95% purity) and TiB₂ (99.9% purity) were used for the sintering of either Ti/TiB (with hcp Ti matrix) or Ti-15wt.% Mo/TiB (with bcc Ti matrix) composites. The average sizes of the Ti, Mo and TiB₂ particles in the powders were 25, 20 and 4 μm, respectively. The powders mixture containing 90 wt.% Ti and 10 wt. % TiB₂ (to obtain the Ti with 17 vol.% of TiB) or 80.75 wt.% Ti, 14.25 wt.% of Mo and 5 wt.% of TiB₂ (to obtain a Ti-15wt.% Mo alloy with 8.5 vol.% of TiB) were produced using a Retsch RS200 vibrating cup mill in ethanol for 1h; the milling rotation speed was 700rpm.

Specimens of Ti/TiB and Ti-15Mo/TiB MMCs, measured 19 mm diameter and 20 mm height, were produced through the SPS process using a Thermal Technology SPS10-3 machine under vacuum at 40 MPa for 5 min at 1000 °C (Ti/TiB) or 1200 °C (Ti-15Mo/TiB).

Discs measured 0.7 mm thickness and 10 mm diameter were deformed by HPT at 400 °C and 6 GPa with a speed of 1 rpm. The maximum shear strain was $\gamma=157$ (5 rotations). The corresponding shear strain level γ can be calculated as [7]: $\gamma = \frac{2\pi Nr}{h}$, where N is the number of revolutions, r is the radius and h is the thickness of the specimen.

X-ray diffraction (XRD) analysis was done for the shear plane of the specimens using an ARL-Xtra diffractometer with CuK_α radiation. The structure and mechanical properties were studied in the mid-thickness of the specimens in the axial cross-section (SEM and microhardness) or in the shear plane (TEM). Vickers microhardness was determined as the average of at least 10 measurements under a load of 1 kg for 10 s.

3. Results and discussion

3.1. Initial microstructure

XRD showed that Ti/TiB MMC (figure 1a) consisted of hcp α -Ti (78.6 vol.%), TiB₂ with a hexagonal lattice (2.4%), and TiB with an orthorhombic lattice (19%). Ti-15Mo/TiB MMC (figure 1b) contained a β -Ti solid solution with a bcc lattice (84 vol.%), α'' martensite with an orthorhombic lattice (4%), TiB with the orthorhombic lattice (10%) and retained TiB₂ with the hexagonal lattice (2%).

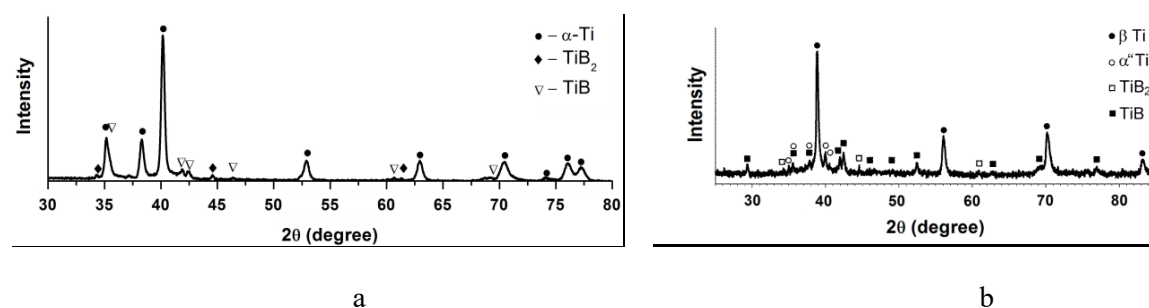


Figure 1. XRD patterns of the Ti/TiB (a) and Ti-15Mo/TiB (b) MMCs.

The microstructure of the Ti/TiB composite was also presented by three structural components: the Ti matrix, TiB whiskers and retained TiB₂ particles (figure 2a). The average diameter of the TiB whiskers was 36±15 nm. TEM showed TiB non-uniformly distributed whiskers in the matrix (figure 1b). The microstructure of the Ti-15%Mo/TiB composite qualitatively similar to that obtained in Ti/TiB, however the average diameter of TiB fibers was founded to be noticeably higher (~130 nm).

The dislocation density was quite high, especially in the Ti/TiB composite with a higher content of TiB; however, in some places single TiB whiskers can be recognized (figure 2 b, c). Grain boundaries were not seen in the microstructure of both MMCs. Meanwhile, the inter-TiB-whiskers-spacing, which determines the free dislocation path was $\sim 1.5 \mu\text{m}$. The volume fraction of pores in the structure of both composites did not exceed 0.5%. It should be noted also that some variations in the Mo percentage were detected in the bcc matrix of the Ti-15%Mo/TiB composite ($\pm 3\%$ around the nominal Mo content of 13.5 wt.%).

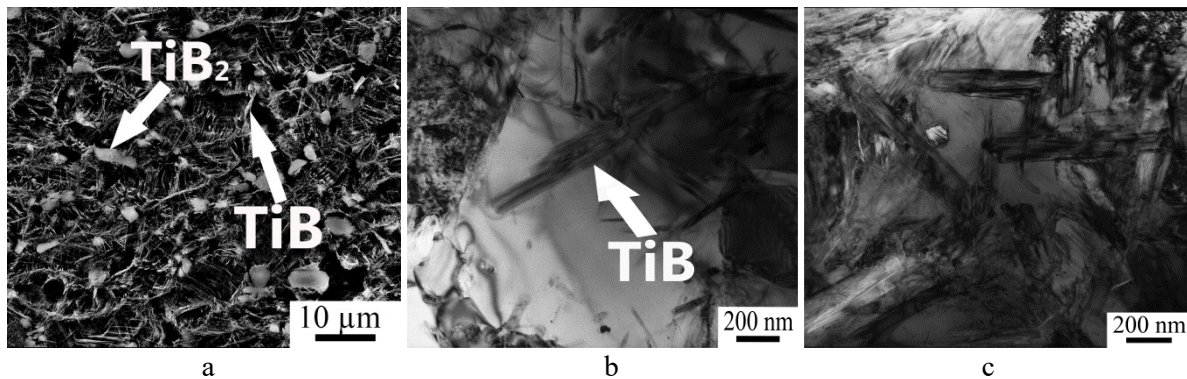


Figure 2. Initial microstructure of Ti/TiB (a,b) and Ti-15%Mo/TiB (c) composites (a) - SEM (etched surface) and (b, d) - TEM images.

TEM images of the severely deformed composites are shown in figure 3. In both composites, the matrix microstructure was refined considerably after HPT to 5 revolutions with the formation of dense dislocation arrays, cells and (sub)grains. The size of the strain-induced cells and (sub)grain was evaluated to be $\sim 30 \text{ nm}$ in Ti/TiB or $\sim 50 \text{ nm}$ in Ti-15%Mo/TiB. In addition, the Mo distribution throughout the Ti-15%Mo/TiB composite microstructure was found to be quite uniform after HPT.

The TiB whiskers were also refined considerably during HPT. Debris measured of 150-300 nm in length were found in both composites suggesting the formation of modestly elongated (the l/d aspect ratio was ~ 10 in the case of Ti/TiB) or nearly equiaxial ($l/d \approx 1.5$ in Ti-15%Mo/TiB) particles.

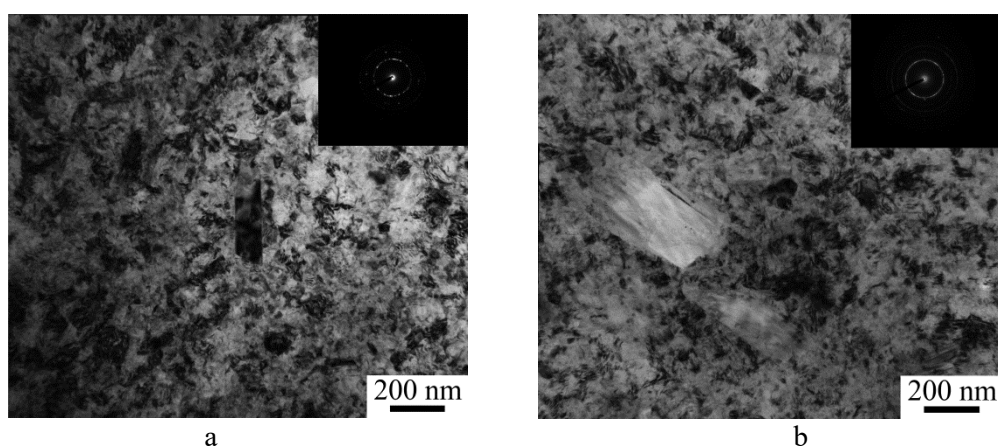


Figure 3. Bright-field TEM images of Ti/TiB (a) and Ti-15%Mo/TiB (b) after five HPT revolutions ($\gamma \approx 157$).

The microhardness analysis shows a considerable hardening of both composites during HPT (figure 4). The increase in hardness at the edge (figure 4b) was expectably more intensive than that in the center (figure 4a) in both composites. On the other hand, the response of Ti-15%Mo/TiB hardness on

strain was more pronounced both in the center and at the edge in comparison with that of Ti/TiB. In addition, the initial level of the microhardness was noticeably higher in Ti-15%Mo/TiB irrespective to two times lower fraction of TiB (8.5 vol. % vs. 17%).

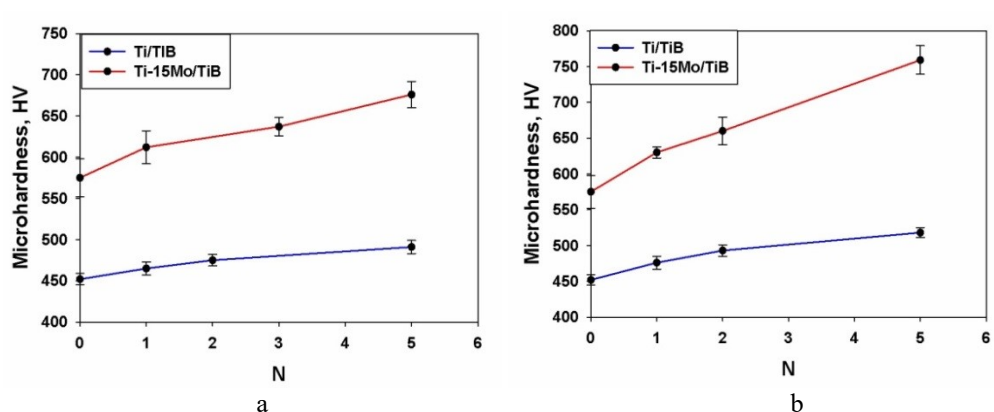


Figure 4. Microhardness evolution of the Ti/TiB and Ti-15%Mo/TiB MMCs during HPT at 400°C in the center (a) and at the edge (b) of the discs.

The latter was most probably associated with a higher contribution of solid-solution strengthening. Other main factors which contributed to the overall strength of the severely deformed composites are Hall-Petch strengthening and precipitation hardening (considering dislocation density similar in both composites). A rough estimate showed that after 5 revolutions of HPT, the main contribution into the strength was associated with precipitation hardening via the Orowan mechanism (~60% in both composites) although the absolute value was higher in Ti-15%Mo/TiB. Hall-Petch strengthening and substructure (dislocation) hardening were noticeably low, giving together ~40% contribution.

4. Conclusions

The microstructure and microhardness evolution of the Ti/TiB and Ti-15Mo/TiB composites were studied during HPT at 400 °C to a strain of $\gamma=157$. The following conclusions were drawn:

- i) Five revolutions of HPT resulted in the microstructure with a (sub)grain size of ~30 or 50 nm in Ti/TiB or Ti-15%Mo/TiB, respectively. The length of the TiB whiskers decreased to 150-300 nm.
- ii) The microhardness increased from 445 HV in the initial state to 510 HV after 5 revolutions and from 575 HV to 730 HV in the Ti/TiB and Ti-15Mo/TiB composites, respectively.

Acknowledgments

The work was supported by the Russian Science Foundation under Grant № 15-19-00165. The authors are also grateful to Joint Research Center “Materials and Technologies”, Belgorod State University, for the assistance with instrumental analysis.

References

- [1] Valiev R Z, Islamgaliev R K and Alexandrov I V 2000 *Progr. Mater. Sci.* **45** 102
- [2] Ovid'ko I A, Valiev R Z and Zhu Y T 2018 *Progr. Mater. Sci.* **94** 462
- [3] Khorasani A M, Goldberg M, Doeven E H and Littlefair G 2015 *Journal of Biomaterials and Tissue Engineering* **5** 593
- [4] Morsi K 2019 *J. Mater. Sci.* **54** 6753–6771
- [5] Ozerov M, Klimova M, Kolesnikov A, Stepanov N and Zhrebtsov S 2016 *Mater. Des.* **112** 17
- [6] Ozerov M, Klimova M, Sokolovsky V, Stepanov N, Popov A, Boldin M and Zhrebtsov S 2019 *J. Alloys Compd.* **770** 840
- [7] Zhilyaev A P and Langdon T G 2008 *Prog. Mater. Sci.* **53** 893